Plasma-induced physicochemical effects on a poly(amide) thin-film composite membrane

Rackel Reis [a*], Ludovic F. Dumée [b], Andrea Merenda[b], John D. Orbell[a], Jürg A. Schütz[c] and Mikel Duke[a]

[a] Institute for Sustainability for Innovation, College of Engineering and Science, Victoria University, Hoppers Lane, Werribee, VIC 3030, Australia

[b] Institute for Frontier Materials, Deakin University, Pigdons Road, Waurn Ponds,VIC 3216, Australia

[c] CSIRO Manufacturing, 75 Pigdons Road, Waurn Ponds, VIC 3216, Australia

***** Author to whom correspondence should be addressed: rackel.reis@live.vu.edu.au

Abstract: Helium and water gas plasma were used to modify the surface morphology and chemistry of commercial thin film composite membranes. Such surface treatment is a convenient tool to alter performance of the membranes and subsequently reduce interactions with contaminants in solution. Plasma reactions such as etching and re-deposition resulted in surface functionalization and texturation which were correlated with membrane flux and salt rejection changes. Investigations conducted using atomic force microscopy revealed morphology alterations which were apparent as either smoother surfaces or rougher surfaces. While the smoothing was attributed to a re-deposition of polymer material, which originated most likely from vaporization of surface polymer, the roughening was a result from balanced plasma surface reactions. The beneficial etching can occur under certain conditions when helium is used in conjunction with low excitation power, which resulted in flux enhancements up to 66% (i.e. from 30 $L.m^{-2}.h^{-1}$ to 50 $L.m^{-2}.h^{-1}$) with 98 % rejection. The hydrophilicity was dramatically increased from 46.6° to as low as 8.9° after 5 min of helium plasma duration. The impact of plasma treatments have on the nascent structure was discussed in order to highlight its application as a convenient tool to functionalize the surface of thin film composite membranes.

Keywords: Plasma gas surface modification, hydrophilicity control, surface texturation, flux enhancement, thin film composite membrane

Graphical abstract

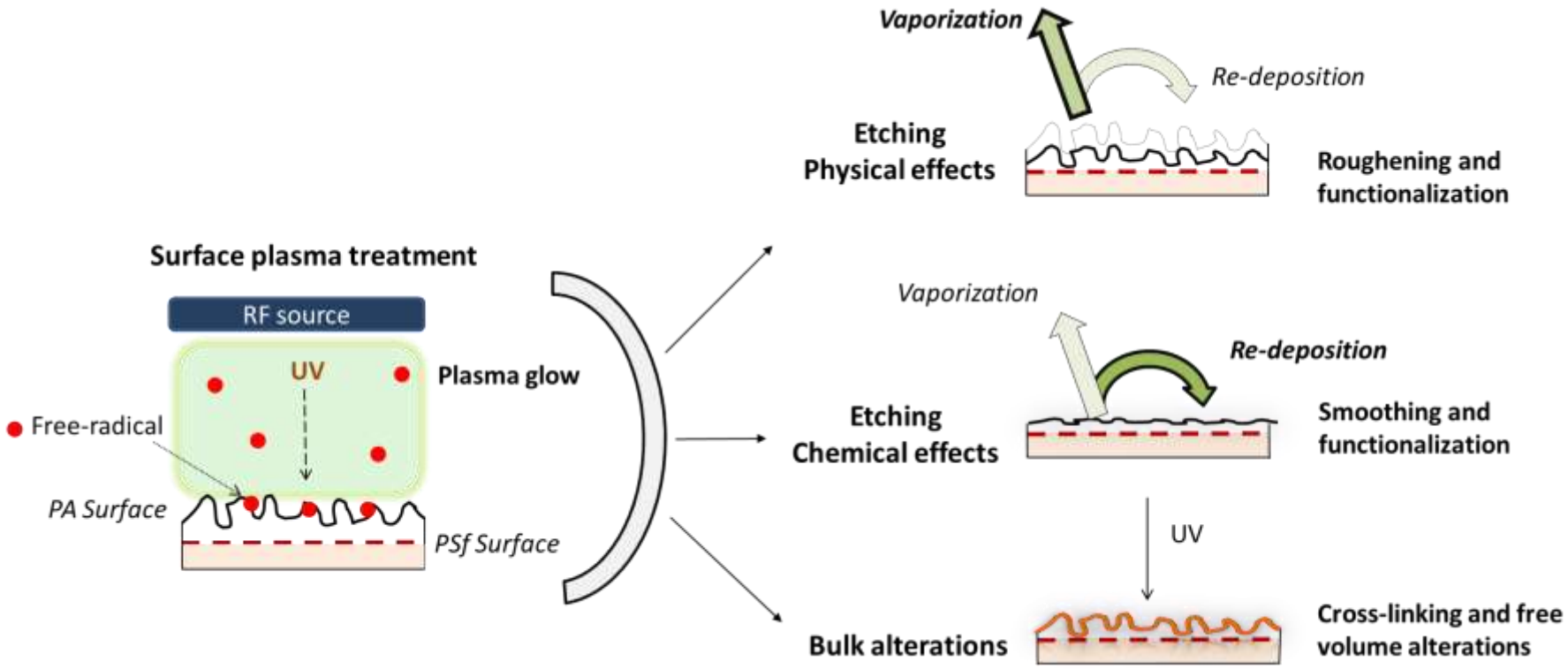

1. Introduction

Thin film composite (TFC) membranes have become benchmark materials for applications in nano-filtration (NF) or reverse osmosis (RO) technologies. These membranes represent a performance-breakthrough with the combination of flux and selectivity in desalination membranes. However, despite such phenomenal industry take-up over the last 30 years, membrane damage incurred by fouling and bio-fouling still remains a key challenge [1, 2]. These issues are limiting membrane performance and lifespan due to the varying water quality which impacts negatively on operating costs of desalination plants. The design of advanced surfaces is therefore a key to sustaining long term performance during operation and to managing the adverse and unavoidable effects of fouling [3]. Surface modifications of TFC membranes are viable routes to custom design TFC membranes. Chemical routes have been mainly targeted towards controlling surface hydrophobicity and roughness through chemical grafting and surface coating [4-7]. Increasing the hydrophilicity of the surface will reduce its affinity with organic foulants [8, 9], while reducing surface roughness can significantly decrease physical adhesion of foulants and suppress solid deposition on the surface [10, 11]. Although chemical grafting and surface coating were shown to reduce fouling, in practice such conventional chemical techniques add to operating costs due to the use of large amount of chemicals and additional treatment steps [12-14]. Novel cost-effective routes are therefore sought to manufacture surface energy tunable materials with enhanced performance.

Plasma chemistry is a rapidly developing technique with low environmental impact [15-17]. This versatile technique uses reactants in the form of gases or vapors to create distinct and systematic alterations of material surface properties from short treatment times [15]. High frequency plasmas operating at 13.56 MHz and low pressures ($\leq$ 100 Pa) are particularly well

suited for treating thin membrane structures due to excellent uniformity of the resulting treatment and the absence of hot arcs, which can burn holes [18, 19]. Most investigations involving plasma treatments have focused on modification of ultra- or micro-filtration membranes [20-22] and utilized a range of reactant gases. In this regard, water (H_2O) and helium (He) plasmas are cost effective reactants for tuning the membrane surface morphology and graft favorable bonding functionality for subsequent processing [23, 24]. Although some benefits of plasma in membrane technology are well established, only few studies have explored applying such plasma treatments to poly(amide) (PA) TFC membranes [25-27]. The PA chemical structure is by nature a highly cross-linked and hierarchical material which therefore several synergistic effects work in unison to achieving an exemplary desalination performance. Experimental parameters (i.e. reactant gas, working pressure and excitation power) are sought to be adjusted considering the specific nature of PA membrane structure in order to achieve an optimal balance of surface modifications without compromising performance [28].

Some plasma reactions may cause different impacts on PA structure which can be beneficial if parameters are well controlled. For instance, electron-initiated reactions from RF plasmas may activate and simultaneously generate free-radicals from reactants as well as from polymer material of the treated substrate. Exposure to air after plasma treatment in general creates more hydrophilic surfaces by incorporation of low-molecular weight oxidized structures and subsequently improving anti-fouling properties [29, 30]. In addition, some plasma treatments of polymeric membranes have been demonstrated to simultaneously increase surface hydrophilicity and roughness which potentially contributed to flux enhancement during organic fouling operation tests [25, 31, 32]. Collisions of electrons at certain angles to the material surface also cause bond scissions, which remove material from the vicinity of the surface via a process known as ‘etching’[28]. Simultaneously, as materials

are removed from the surface, re-deposition of the same materials in vaporized phase may occur [33, 34]. On the other hand, intense plasma conditions, such as high excitation power and long duration, may favour some undesired reactions which can suppress functionalization mechanisms. Therefore the adjustment of the excitation power is critical to controlling the extent of etching on the surface. Such mechanisms are governed by UV emissions present in RF plasma, and therefore the treated material's inherent UV absorption capacity may strongly facilitate such reactions [35]. For example, UV absorption in PA occurs mainly in the vicinity of 300 nm wavelength [36]. Intense UV absorption may lead to excessive re-deposition, cross-linking and branching of macromolecules which can potentially penetrate as far as 200 nm into the PA layer. The resultant process may reduce surface area [37] and create membrane resistance, a similar issue also found in surface coating modifications [4, 13, 38] which can also impact on membrane flux [15, 39].

In this work, for the first time, commercial TFC membranes were treated with pure He and H_2O gas plasma for a broad range of excitation power and exposure durations. The plasma powers were therefore chosen to cover a broad range of potential plasma excitation energies, as well as different levels of emitted UV light, from the plasma glows. The investigation also sought to evaluate their impact on the material's morphology, surface energy and microstructure, being parameters known to affect membrane performance. This study gives in-depth insights into membrane performance associated with plasma surface reactions contrasted by two divergent gas reactants. The modified membranes were characterized and potential practical improvements for desalination performance were discussed.

2. Experimental Section

2.1 Reagents and materials

BW30 TFC membranes were purchased from Dow Filmtec Corp. (IMCD limited Australia). The TFC RO membrane is a multilayer material composed of an extremely thin active (~100-200 nm) and semi-dense layer of PA. This layer is deposited on top of a thick porous support substrate (e.g. poly(sulfone) (PSf)) coated on to a nonwoven (e.g. poly(ester) (PES)) fabric structure [2]. Membranes were conditioned prior to plasma processing by immersing them in deionized (DI) water for 5 hours, dried in air and then rinsed with ethanol prior to permeation. This procedure represents the common activation process for new membranes of this type.

2.2 Plasma treatments

Plasma treatments were performed using a low pressure plasma system from Diener Plasma Surface Technology, model Pico-RF-PC and operating in the high frequency band at 13.56 MHz. Reactants were water H_2O and He, which were injected into a 7.7 L stainless-steel chamber at a constant pressure of 0.2 mbar and exposed to either 10 W or 80 W excitation power for a duration of 1, 2 or 5 min. Immediately after plasma treatment the membranes were purged in nitrogen for 20 seconds in order to avoid oxidation in air and better preserve the chemical modification.

2.3 Characterization techniques

2.3.1 Scanning Electron Micrographs (SEM)

SEM images were obtained from a Quanta dual beam Gallium (Ga) Focus Ion Beam (FIB) Scanning Electron Microscope from FEI and samples were coated with carbon prior to image

analysis. Images were collected at 20 keV acceleration voltage with a working distance of 10 mm.

2.3.2 Atomic Force Microscopy (AFM)

Atomic force microscopy (AFM) analysis was performed in tapping mode using a Bruker model Nanoscope V with multimode scanning capability and equipped with a microscope camera 10xA Nikon series 110422 to monitor the scanning area. The resonance frequency and force constant of the cantilever probe was 300 kHz (±100 kHz) and 40 N/m, respectively. Data was collected using Nanoscope 8.4 software, providing a scan window size of 7 µm. Images were subsequently evaluated using Gwyddion.36 data analysis software. The accuracy of plotted data sets was within a 95% confidence interval of the true value.

2.3.3 Contact angle

Contact angle measurements were performed with a Biolin Scientific goniometer to map differences in hydrophobicity across the membrane surface. Contact angle measurements were performed 1 hour after plasma treatment. Each test involves applying 4 µL of de-ionized water in the form of drops in three different spots on the membrane surface. Images were acquired 5 seconds after application of the water drop and contact angles were calculated by fitting the image of the drops using the Young-Laplace algorithm from the optical tensiometer software. Plotted data lies within the 95% confidence interval of the true value.

2.3.4 Attenuated Total Reflection-Fourier Transform Infrared Spectroscopy (ATR-FTIR)

Analysis of surface functional groups created by the plasma treatments was performed using a Perkin Elmer infrared spectrometer, model Frontier with KBr beam splitter and diamond ATR crystal. All spectra were collected across a wavenumber range of 4000-850

cm^{-1}, 8 spectra were averaged at resolution of 4 cm^{-1} and analyzed with OPUS 7.2 software from Bruker Corporation.

2.3.5 X ray photoelectron spectroscopy (XPS)

X-ray photoelectron spectroscopy (XPS) was utilized for surface and interface characterization. XPS was performed using a Thermo Scientific™ K-Alpha+™ X-ray photoelectron spectrometer. The photon energy was 1253.6 eV, line width 0.7 eV and Mg K_{alpha} hv=486.7 nm filament. A quantitative elemental composition of the modified PA was provided for a surface depth of 1–5 nm and detection limit of 0.1% of the bulk material. The peak position was calibrated using the C1s peak at 284.6 eV.

2.4 Membrane performance

Salt rejection and water permeation performance were tested with a laboratory-scale cross-flow filtration system model CF042 from Sterlitech Corp., WA, USA. The circulating feed stream contained 2,000 mg/L of sodium chloride (NaCl) from Sigma Aldrich (99% purity) at 25°C. The effective membrane area was 42 cm^2 and the trans-membrane pressure was monitored and maintained at the target working pressure of 15 bar within +/- 2% accuracy. The circulating permeate flow at the outlet was collected after 2 h and salt rejection conductivity measured immediately on completion of the test. Salt concentration was determined using an electrical conductivity meter (Hach HQ40d) and permeate mass was measured using a balance with a resolution of 0.001 grams. Data acquisition software was used to record the permeate flux for a 1 min interval. Each desalination test was replicated twice and error bars of about 7% were obtained after considering the estimated standard error of the mean values.

Salt rejection R (%) was calculated according to:

$$R = 1 - \left(\frac{C_p}{C_f}\right) \times 100\% \quad (1)$$

where C_p and C_f are measured conductivities of the collected permeate and initial feed (in µS/cm), respectively, which represent the corresponding salt concentrations, assuming that the conversion between conductivity and concentration is linear within corresponding concentration ranges. Total permeate flux J_w (L.m^{-2}.h^{-1}) was calculated by:

$$Jw = \frac{V}{A \times t} \quad (2)$$

where V is volume of the permeate (L), A is effective membrane area (m^2) and t is time in hours over which the volume V was collected.

3. Results and Discussion

3.1 The impact of plasma treatments on membrane performance

The impact of various plasma treatment conditions on membrane performance, including the total flux and salt rejection, were investigated first. The total water flux and salt rejection of various treated membranes, as measured in a cross-flow set up, is displayed in Figure 1 as a function of the nature of etchant gas, excitation power and process duration. The use of NaCl solution is a standard procedure to investigate the integrity of the PA layer after plasma modification. Although other salts may have been selected, the small kinetic diameter of Na^+ ions as well as the single charge on both ions is pertinent properties for the testing of the integrity of the material. Flux for the untreated reference membrane was 30 L.m^{-2}.h^{-1}, and is indicated as the first bar on each of the sub-figures. NaCl salt rejection was 97%. These levels of flux and rejection are typical for state of the art brackish water TFC membranes provided by the supplier [40].

The flux through the membranes after H_2O plasma treatment at 0.2 mbar and 10 W was found to be statistically similar to that of the reference membranes at any plasma treatment duration with no significant loss in salt rejection, as shown in Figure 1. At 80 W, however, the flux was significantly reduced after 2 min of plasma treatment, while rejection remained unaffected in comparison to the control membrane. At the longer treatment time of 5 min, a sharp loss in salt rejection was observed, declining to 84%. Conversely, the permeation of He plasma treated membranes at 10 W showed systematic flux increases as a function of the exposure duration while simultaneously exhibiting slight rejection loss. The flux for the 1 and 2 min treated samples improved by up to 17%, and up to 66% for the 5 min treated membrane. At 80 W of plasma excitation power the flux of He plasma treated membranes declined, while rejection remained approximately constant at 98.8 ± 0.5 %.

Resultant processes produced vastly different outcomes as a function of both exposure duration and excitation power. In order to understand the effect of plasma treatments on the modified surface, further physico-chemical characterization of modified membrane surface is required to explain the observed increases in permeation.

3.2 Membrane characterization

Competitive plasma surface reactions arise from the etching processes, which can lead to differing degrees of surface functionalization and roughening [41]. If plasma conditions are intensified, a net re-deposition of vaporized materials can result in the surface becoming smoother by cross-linking and free volume densification [33].

Etching promotes bond scission processes [42] and simultaneously, chemical bond reformation may lead to texturation and roughness changes on the membrane surface. Bond reformation may be confined to the outermost PA layer and present as temporary surface functional groups. However, with increasing penetration depth within the PA layer, and

188 further stimulated by UV light from the plasma, the process can result in internal PA cross-
189 linking [33, 34]. Chemical effects from etching, in conjunction with re-deposited, vaporized
190 materials, may also occur as a result of high excitation power and long exposure time, which
191 leads to reduced surface roughness. Oxidative gases can especially promote aromatic rings
192 scissions [43, 44] and lead to severe PA degradation due to potential polymer backbone bond
193 scissions [45].

194 The interplay of these competing effects is believed to be at the core of experimental
195 observations made and is discussed in the following in terms of physical and chemical
196 changes occurring on the membrane.

197 **3.2.1 Morphology characterization of the plasma modified membranes**

198 Initial investigations of morphology changes were performed by acquiring SEM images of
199 the membrane surfaces as a function of the treatment conditions. Figure 2a shows the SEM of
200 the control membrane [46]. As shown in Figure 3, the surface of the H_2O treated membranes
201 was significantly smoothed with increasing treatment duration, with the effect intensified for
202 higher excitation power. In contrast, the topographical SEM analysis for He plasma in Figure
203 4 shows that modified membranes at 10 W were slightly smoothed for short plasma
204 treatments, while roughening occurred for a treatment time of 5 min. The same effect was
205 also found at 80 W.

206 In order to confirm topology variations found by SEM, the average roughness (Ra) for
207 the modified membranes was measured by AFM and compared with a control membrane with
208 Ra of 63 nm (Figure 2b). As shown in Figure 5 and Table S1, H_2O treated membranes at 10
209 W showed reduced Ra from 63 nm (control) down to 43 ± 2.6 nm after only 1 min of plasma
210 treatment. Beyond 1 min, the roughness values increased back up to Ra 57 ± 5.0 nm between
211 2 and 5 min. At 80 W increased plasma durations led to increased smoothing effect with Ra

reduced down to 57 ± 2.5 nm at 1 min, to 36 ± 2.2 nm at 2 min, and then 47 ± 4.3 nm at 5 min. Previous studies on CO_2 plasma treatment of poly(ether sulfone) (PES) membrane also demonstrated that smoothed morphologies were achieved for the treated surfaces [47]. The SEMs showed that between 1 to 5 min of plasma treatment pores were gradually reduced in diameter and progressively disappeared. However, beyond 5 min, the pore size started to increase again and to reappear across the surface. The alterations of pore diameters were attributed to etching and re-depositions on the surface. Interestingly, the etching rate was found to be largely depending on the power density than the re-deposition rate for this material.

Here, the smoothing was not consistent with He plasma treatment, as shown in Figure 6 and Table S2. At 10 W there was a progressive roughening trend, similar to that reported for the SEM analysis. For shorter treatment durations, between 1 and 2 min, the roughness was slightly reduced to 60 ± 0.5 nm and 58 ± 1.2 nm. However, a significant roughening effect was observed with longer plasma treatment, with Ra increasing to 70 ± 1.5 nm at 5 min which is in good agreement with previously reported study [48]. A similar roughening effect was observed with helium plasma (25 W) treatment on PES membranes. Significantly increased roughness values were measured from 11 nm (control) to 39 nm after 30 s of plasma treatment duration. Although these roughening mechanisms may be attributed to fragments of re-deposited materials, the exact mechanisms involved were not conclusive to date [48]. He plasma at 80 W, however, showed a smoothing trend, stronger than observed for water plasma, with Ra reduced to around 40 ± 2.7 nm for all durations which therefore may be attributed to re-deposition of molecular fragments of removed materials.

Increased resistance to water flux through the PA layer promoted by H_2O plasma (i.e. decreased water fluxes observed in Figure 1) may be due to a potential densification of the free-volume in the selective layer [49, 50]. A similar mechanism may have occurred for He

plasma at 80 W. In this regard, the use of He at 10 W appeared to provide successful etching with balanced plasma conditions [45] resulting in increased surface area, which contributed to the flux enhancement shown in Figure 1. Material hydrophobicity also plays a role in altered membrane performance [51, 52] and further chemical analysis is needed.

3.2.2 Chemical characterization of the plasma modified membranes

Investigation of the chemical functional group changes across the membranes was performed by ATR-FTIR analysis. Variations in absorbance from studied frequencies (described in Table S3) showed potential degradation and functionalization of aromatic rings in the polymer backbone.

The analysis of the FTIR spectra (Figure 7) for H_2O plasma modified membranes showed that absorbance decreased with the broadening of the band at 3330 cm^{-1}, corresponding to N-H and OH groups stretching vibration, for both 10 W and 80 W. This effect is an indication of chemical degradation commonly found with oxygen containing plasmas [41]. Although a broadening peak was observed at both power intensities, possible etching at 80 W suggests an intensified physical erosive behavior, confirmed with significant salt rejection loss with only 84 % after 5 min of treatment (Figure 1).The bands at 1663, 1609 and 1541 cm^{-1} generally showed similar absorbance patterns for both 10 and 80 W. However, a functionalization reaction at longer exposure time (5 min at 80 W, Figure 7) showed a new carbonyl band around 1734 cm^{-1}, attributed to post-plasma reactions with unreacted radicals or peroxide radical [41]. These absorbance alterations suggest an ageing process due to a large amount of free-radicals with high excitation power, which can potentially contribute to a hydrophilicity increase.

For He plasma modified membranes, the bands at 3330 cm^{-1} (Figure 8) increased in intensity and some shifted frequencies. At 10 W, the significant increase in intensity for the 5

min duration may indicate functionalization in the amide groups with OH groups [53]. At 80 W, the band shifted to 3400 cm^{-1}, which suggests changes to the neighboring hydrogen bonding [53, 54]. The bands at 1663, 1609 and 1541 cm^{-1} followed similar absorbance patterns for the He plasma at 10W. However, stronger absorbance variations were found at 80 W, which may indicate a potential increase in the etching effect. Therefore, functionalization reactions were more likely to be found with He plasma at low power.

In order to investigate functionalization at the molecular level, an XPS elemental survey analyzed the N/C and O/C ratio. The O/C ratio for H_2O (Table S4) plasma varied slightly, ranging between 0.2 and 0.4. The O/C ratio for H_2O plasma (Table S5) was stable, and may be related to the nature of PA. As the material already has nitrogen and oxygen functional groups in the polymer structure, the incorporation of more of them via plasma treatment will make them very much less visible than with other polymers treated in similar conditions [55]. The N/C ratio increased from 0.03 (control) [56] to 0.1 for both He and H_2O plasmas, with increased excitation power and duration. The nitrogen source is potentially N_2^+ metastable species in the gaseous mixture from residual nitrogen, introduced as purge gas after plasma treatment, since minimal nitrogen concentrations (> 1%) can easily react with aromatic structures due to the inherent electron delocalization from aromatics[57]. Therefore, the increased ratio suggests strong correlations with functionalization, promoted by plasma activation. Details from potential reaction mechanisms were not conclusive.

Functionalization was also investigated using contact angle analysis. Resultant hydrophilicity or hydrophilicity of the outer modified layers can be achieved with morphology [58] or chemical changes [59]. As expected, the contact angle for all plasma modified membranes was significantly reduced (Figure 9). He plasma treatment resulted in consistently lower contact angles for all duration times and power levels compared with H_2O. He plasma also produced more stable contact angle trends.

Competitive processes between functionalization and re-deposition have led to hydrophilicity and morphological alteration, which were correlated with roughness and contact angle. The increased wettability found for membranes treated with H_2O plasma at 10 W showed that with 1 min of plasma treatment the contact angle was well correlated with the decreased surface roughness. After 1 min the resultant hydrophilicity is potentially correlated with the chemical nature of the modified surface, potentially caused by re-deposition of removed materials. Conversely, He plasma at 10 W showed that decreased contact angles were more correlated with reduced roughness for 1 and 2 min durations, with stronger functionalization processes occurring after 2 min. The optimum experimental conditions obtained with He plasma at 5 min duration at 10W suggest a potential treatment for designing membranes with more resistance to protein adhesion (fouling), since hydrophilicity is an important index for antifouling properties of membranes [3, 26, 47, 60, 61]. Intense re-deposition (Figure 9) was more significant at 80 W, where hydrophilicity was better correlated with morphology once roughness was significantly reduced, as well as contact angle. On the other hand, despite the resultant rough surface morphology of the He plasma treated sample and particularly for the 5 min and 10 W treated sample, a significantly reduced contact angle (10.1 ± 2.0^{o}) was measured compared to the control membrane (46.6 ± 3.0^{o}). This lower contact angle may be predominantly related to the re-deposition of etched material on the surface of the membrane. These reconfigured etched materials are very likely to be hydrophilic given the nature and chemistry of the initial membrane material.Therefore, the rougher aspect combined with the functionalization achieved with low contact angles, have preferred water transport for modified membranes. These results are in agreement with other surface modification techniques, such as plasma polymerization and chemical grafting of hydrophilic moieties that increased roughness upon surface hydrophilization with reduced contact angle, which resulted in flux enhancement [34, 62, 63].

4. Conclusions

The impact of H_2O and He plasma on PA surfaces have been investigated. He plasma increased membrane flux by 66% with a 5 min treatment at the lower excitation power of 10 W, without significant loss in salt rejection. At higher power for both gases there was reduced membrane flux, and for H_2O plasma there were physical changes on the surface leading to loss of salt rejection with exposure time. Surface smoothing has been shown to increase the mass transfer resistance of membranes, while significant roughening was achieved with He at 10 W, 5 min, suggesting that plasma under these conditions provided well balanced reactions. Inert gas plasma has been shown to be beneficial in modifying PA material structure. Future work with other inert gases could be explored towards surface tuning and anti-fouling properties.

Acknowledgment

The authors would like to acknowledge a PhD stipend and project funding from the Collaborative Research Network initiative of the Australian Department of Industry. RR acknowledges the postgraduate top up scholarship from the National Centre of Excellence in Desalination Australia, funded by the Australian Government through the National Urban Water and Desalination Plan. Dr. Ludovic Dumée's Alfred Deakin Post-Doctoral Fellowship and Deakin University and the Institute for Frontier Materials Electron Microscopy units.

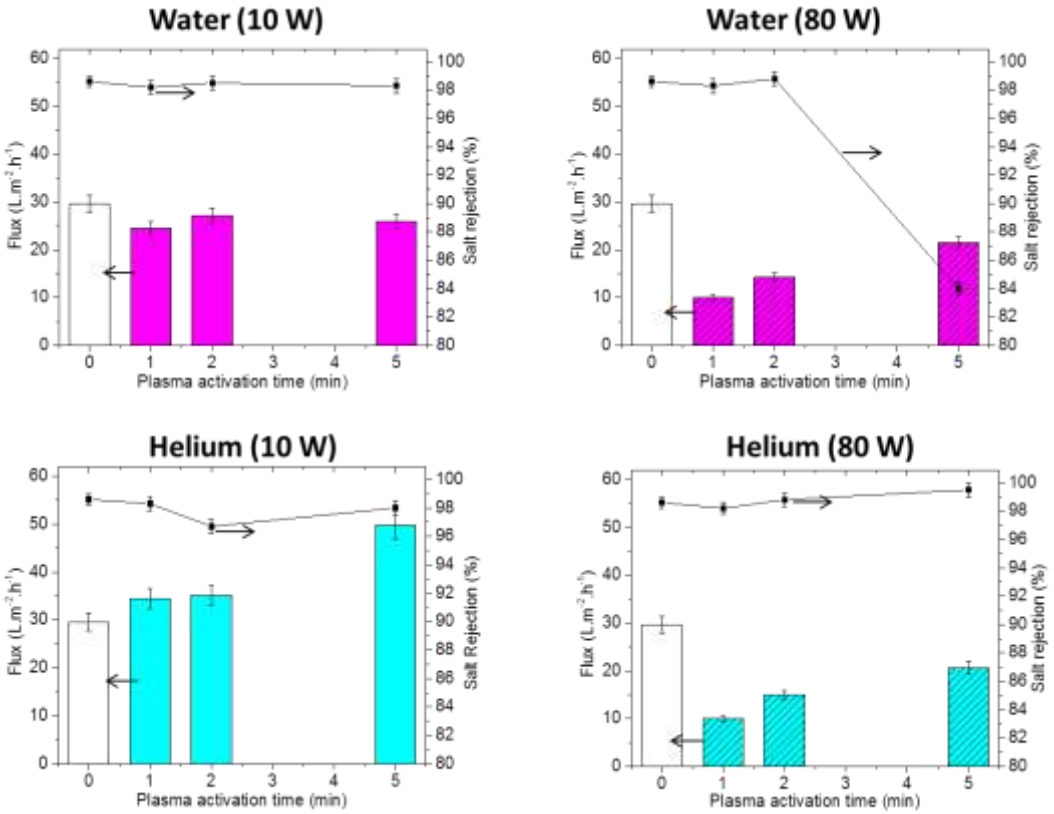

Figure 1: Membrane flux and salt rejection measured after 2 h of testing with 2,000 ppm of NaCl in water at 15 bar feed pressure after plasma modification at 0.2 mbar.

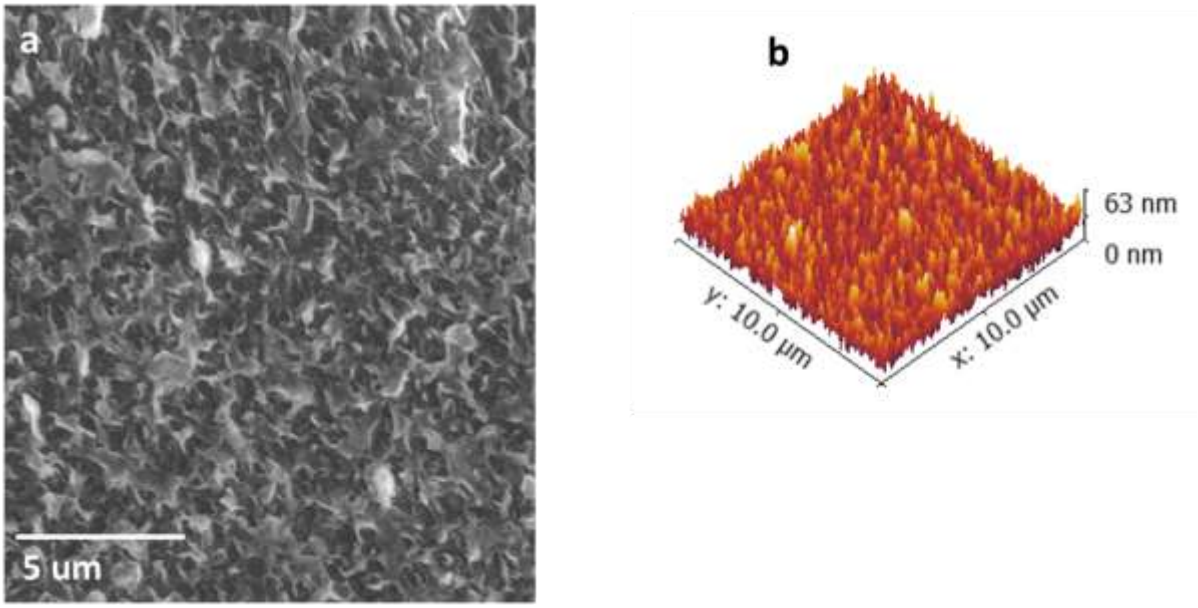

Figure 2: a) SEM image of control membrane and b) AFM analysis of control membrane with Ra 63 nm.

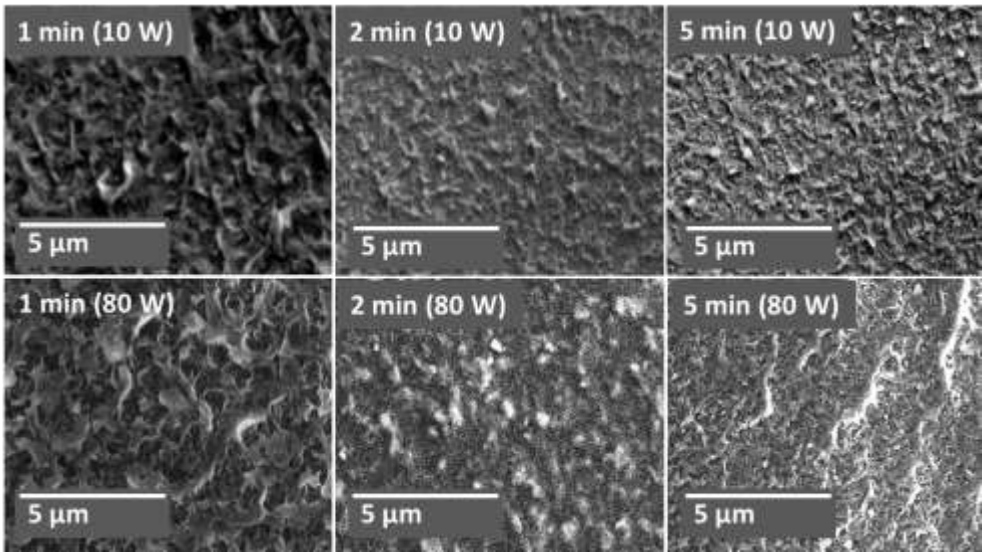

Figure 3: SEM images from H_2O plasma modified membranes.

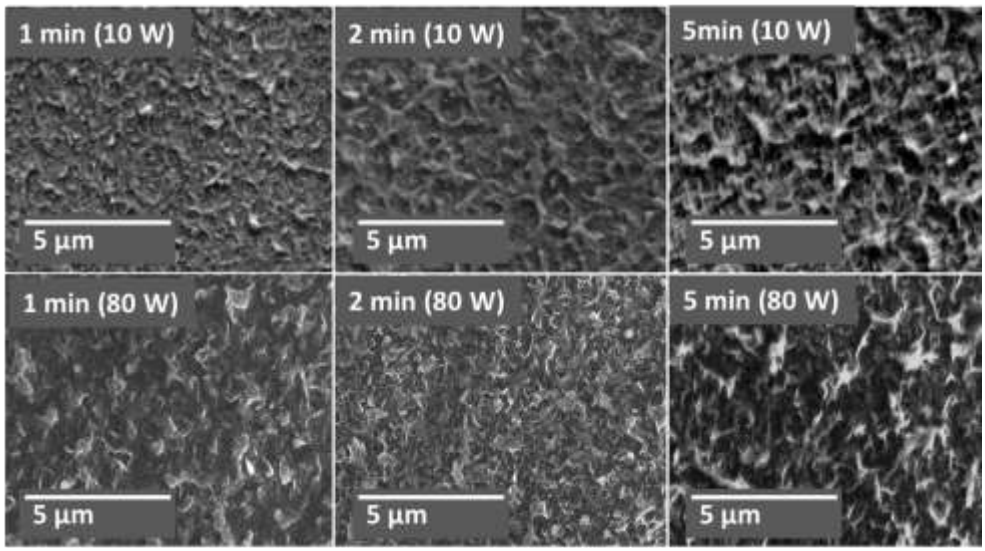

Figure 4: SEM images from He plasma modified membranes.

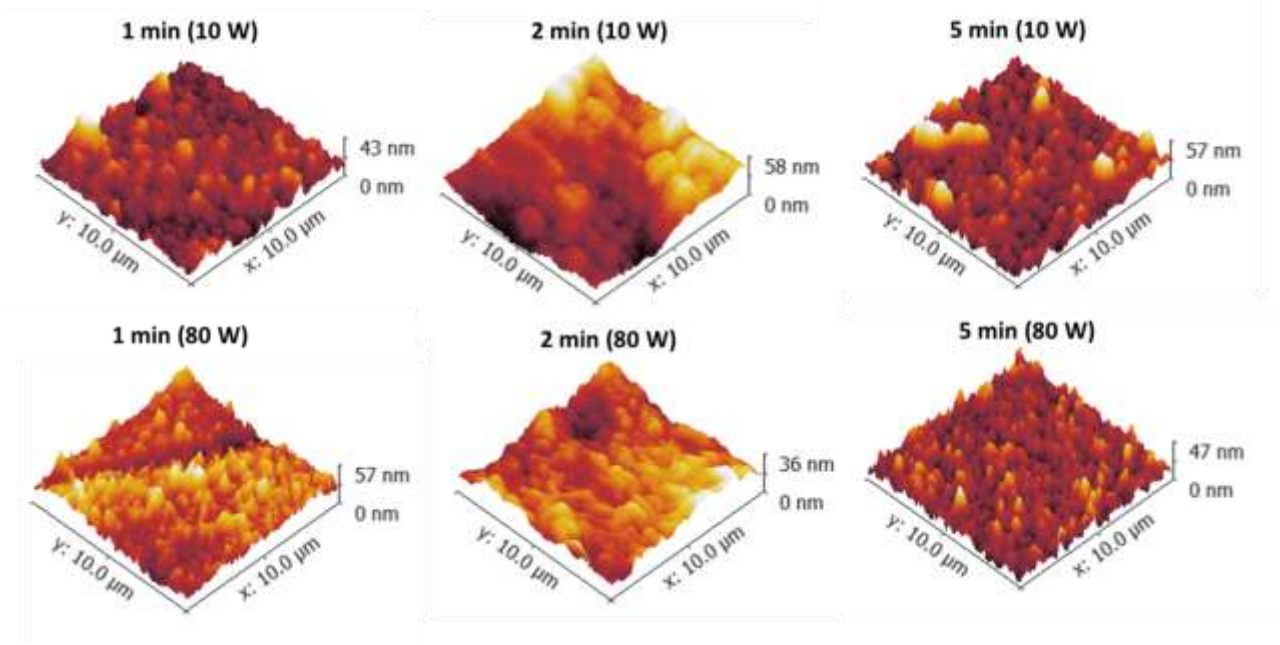

Figure 5: AFM topology mapping H_2O plasma modified membranes.

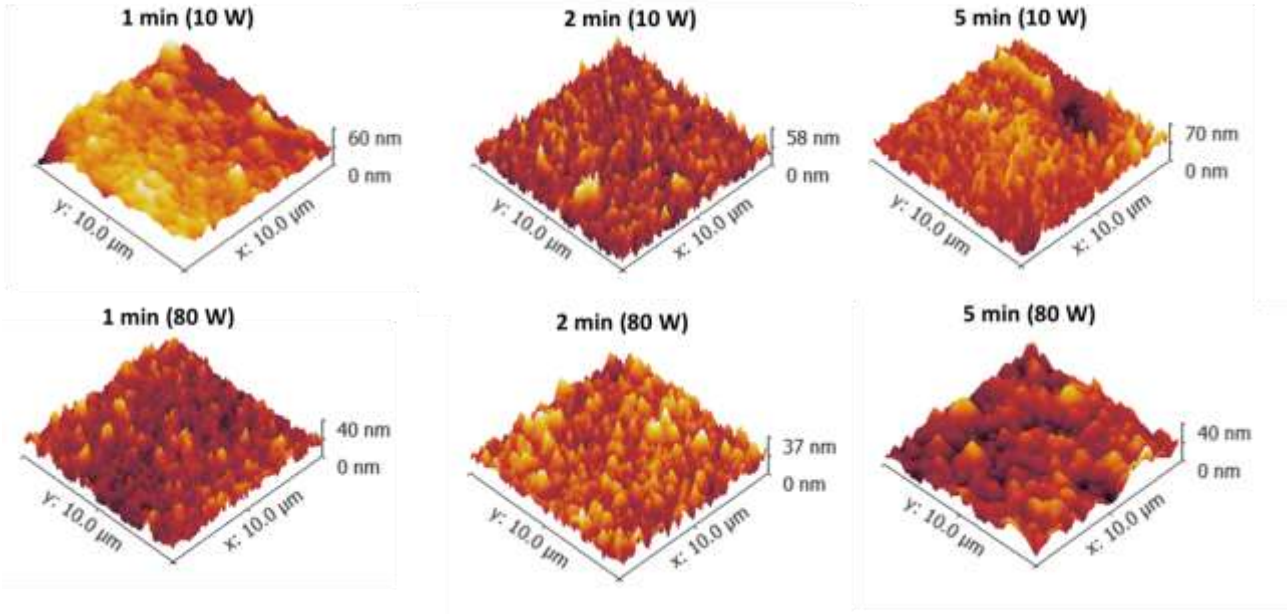

Figure 6: AFM topology mapping for He plasma modified membranes.

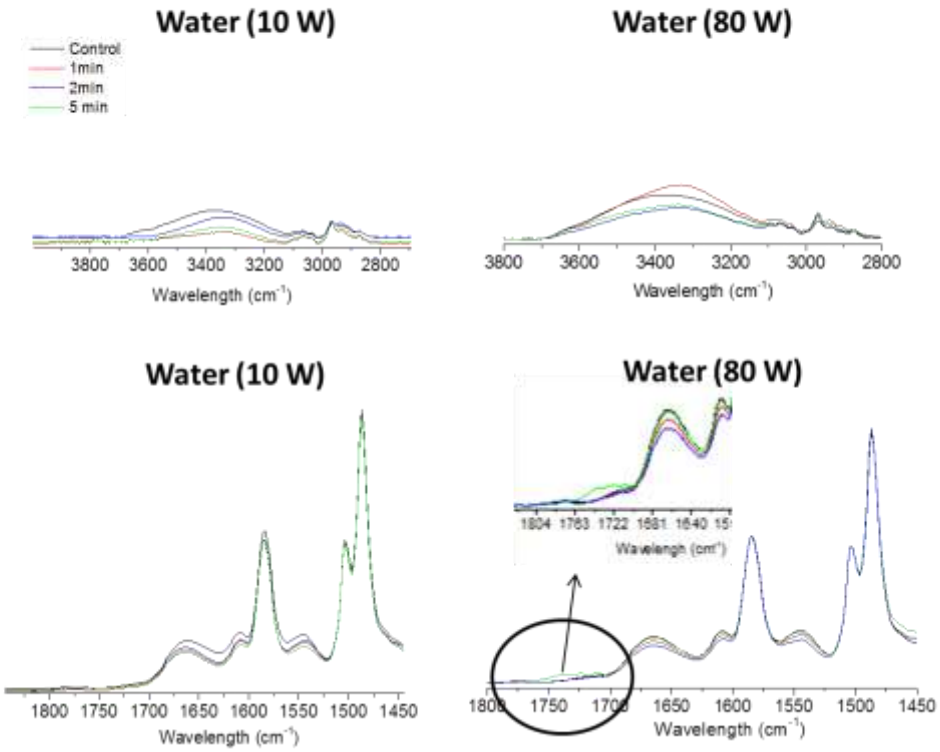

Figure 7: FTIR analysis from H_2O plasma modified membranes: on the top, analysis of N-H and O-H bands at 3330 $cm^{-1}$for modified membranes at 10 W and 80 W; on the bottom, analysis of amide bands from1663 to 1541 cm^{-1} for modified membranes at 10 W and 80 W.

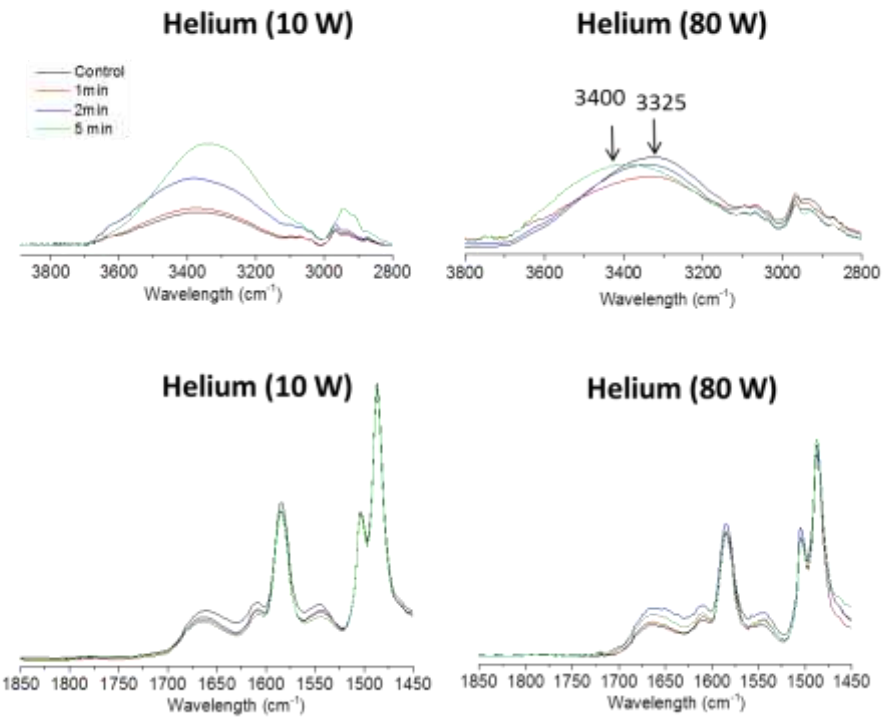

Figure 8: FTIR analysis from He plasma modified membranes: on the top, analysis of N-H and O-H bands at 3330 $cm^{-1}$for modified membranes at 10 W and 80 W; on the bottom, analysis of amide bands from1663 to 1541 cm^{-1} for modified membranes at 10 W and 80 W

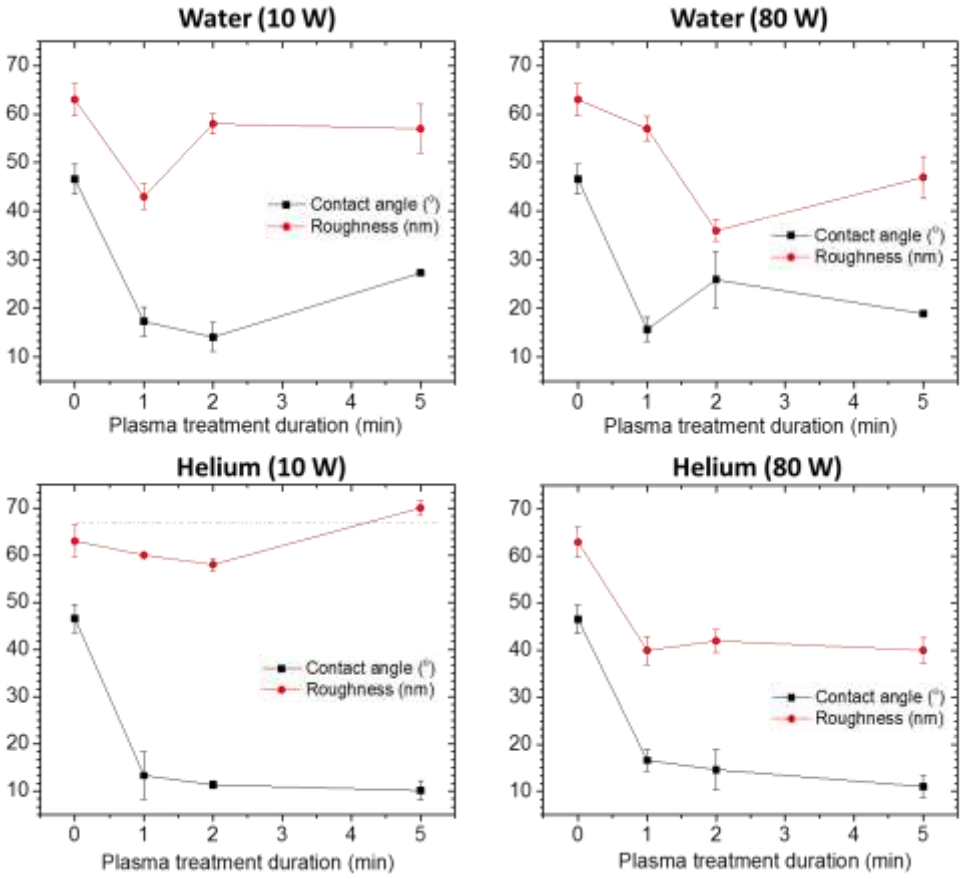

Figure 9: Comparison of contact angle and roughness with increasing time. Each value from contact angle and roughness represents the mean of three measurements in the sample associated with their estimated standard error.

Supplement Material

Table S1: Influence of H_2O plasma on surface roughness and flux

Power density	Membranes	Roughness (nm)	Flux ($L.m^{-2}.h^{-1}$)
-	Control	63.0	30.0
10W	H_2O 1min	43.0	24.0
	H_2O 2min	58.0	27.0
	H_2O 5 min	57.0	26.0
80W	H_2O 1min	57.0	10.0
	H_2O 2min	36.0	14.0
	H_2O 5 min	47.0	21.0

Table S2: Influence of He plasma on surface roughness and flux

Power density	Membranes	Roughness (nm)	Flux ($L.m^{-2}.h^{-1}$)
10W	He 1 min	60.0	34.0
	He 2 min	58.0	35.0
	He 5 min	70.0	49.8
80W	He 1 min	40.0	10.0
	He 2 min	42.0	15.0
	He 5 min	40.0	20.7

Table S3: FTIR and poly (amide) studied frequencies

FTIR frequency (cm^{-1})	**Description**
3330	N-H groups and O-H groups stretching vibration[61]
1663	Amide I band: stretching vibration from the C=O and C-C-N deformation vibration [11]
1609	Aromatic amide N–H deformation vibration or C=C ring stretching vibration [11]
1541	Amide II band: N-H in-plane bending and N-C stretching vibration of a –CO-NH- [53]

Table S4: Elemental XPS analysis from H_2O plasma with increasing N/C ratio [61]

Power density	Membranes	C (at%)	N (at%)	O (at%)	N/C	O/C
	Control	77.5	2.2	20.3	0.03	0.3
10W	H_2O 1 min	80.6	3.3	16.1	0.04	0.2
	H_2O 2 min	84.9	2.1	13.0	0.02	0.4
	H_2O 5 min	72.5	8.1	19.4	0.1	0.3
80W	H_2O 1 min	79.1	5.0	15.9	0.1	0.2
	H_2O 2 min	74.6	6.9	18.5	0.1	0.2
	H_2O 5 min	72.6	8.8	18.6	0.1	0.2

Table S5: Elemental XPS analysis from He plasma with increasing N/C ratio [61]

Power density	Membranes	C (at%)	N (at%)	O (at%)	N/C	O/C
	Control	77.5	2.2	20.3	0.03	0.3
10W	He 2 min	73.3	6.7	20.0	0.1	0.3
80 W	He 5 min	73.8	6.3	19.9	0.1	0.3

References

1. Shenvi, S.S., A.M. Isloor, and A.F. Ismail, *A review on RO membrane technology: Developments and challenges.* Desalination, 2015. **368**: p. 10-26.
2. Cadotte, J.E., Petersen, R.J., Larson, R.E., Erickson, E.E. , *A New Thin-film Composite Seawater Reverse Osmosis Membrane.* Desalination, 1980. **32**: p. 25-31.
3. Lee, K.P., T.C. Arnot, and D. Mattia, *A review of reverse osmosis membrane materials for desalination development to date and future potential.* Journal of Membrane Science, 2011. **370**(1–2): p. 1-22.
4. Yu, S., et al., *Surface modification of thin-film composite polyamide reverse osmosis membranes by coating n-isopropylacrylamide-co-acrylic acid copolymers for improved membrane properties.* J. Membr. Sci., 2011. **371**: p. 293-306.
5. Rana, D. and T. Matsuura, *Surface modifications for antifouling membranes.* Chemical Reviews (Washington, DC, U. S.), 2010. **110**(4): p. 2448-2471.
6. Kang, G., et al., *A novel method of surface modification on thin-film composite reverse osmosis membrane by grafting poly(ethylene glycol).* Polymer, 2007. **48**(5): p. 1165-1170.
7. Cheng, Q., et al., *Surface modification of a commercial thin-film composite polyamide reverse osmosis membrane through graft polymerization of N-isopropylacrylamide followed by acrylic acid.* J. Membr. Sci., 2013. **447**: p. 236-245.
8. Kang, G.-d. and Y.-m. Cao, *Development of antifouling reverseosmosis membranes for water treatment: a review.* Water Research, 2012. **46**(3): p. 584-600.
9. Kulkarni, A., D. Mukherjee, and W.N. Gill, *Flux enhancement by hydrophilization of thin film composite reverse osmosis membranes.* Journal of Membrane Science 1996. **114**(1): p. 39-50.
10. Vrijenhoek, E.M., M. Elimelech, and S. Hong, *Influence of membrane surface properties on initial rate of colloidal fouling of reverse osmosis and nanofiltration membranes.* Journal of Membrane Science 2001. **188**(1): p. 115-128.
11. Tang, C.Y., Y.-N. Kwon, and J.O. Leckie, *Probing the nano and micro-scales of reverse osmosis membranes - a comprehensive characterization of physiochemical properties of uncoated and coated membranes by XPS, TEM, ATR-FTIR, and streaming potential measurements.* Journal of Membrane Science, 2007. **287**(1): p. 146-156.
12. Pan, K., H. Gu, and B. Cao, *Interfacially polymerized thin-film composite membrane on UV-induced surface hydrophilic-modified polypropylene support for nanofiltration.* Polym. Bull. (Heidelberg, Ger.), 2014. **71**(2): p. 415-431.
13. Wu, D., et al., *Modification of aromatic polyamide thin-film composite reverse osmosis membranes by surface coating of thermo-responsive copolymers P(NIPAM-co-Am). I: Preparation and characterization.* J. Membr. Sci., 2010. **352**(1-2): p. 76-85.
14. Belfer, S., Y. Purinson, and O. Kedem, *Surface modification of commercial polyamide reverse osmosis membranes by radical grafting: An ATR-FTIR study.* Acta Polymerica, 1998. **49**(10-11): p. 574-582.

15. Fridman, A., *Plasma Chemistry*. 2008, Cambridge University New York.

16. Borcia, C., G. Borcia, and N. Dumitrascu, *Relating plasma surface modification to polymer characteristics.* Appl. Phys. A: Mater. Sci. Process., 2008. **90**(3): p. 507-515.

17. Sadiqali Cheruthazhekatt, M.C., Pavel Slavicek, Josef Havel, *Gas plasmas and plasma modified materials in medicine.* J. Appl. Biomed., 2010. **8**: p. 55-66.

18. Pethrick, R.A., *Plasma surface modification of polymers: relevance to adhesion*. Polymer International. Vol. 39. 1996: John Wiley & Sons. 79-79.

19. Shenton, M.J. and G.C. Stevens, *Surface modification of polymer surfaces: atmospheric plasma versus vacuum plasma treatments.* Journal of Physics D: Applied Physics, 2001. **34**(18): p. 2761.

20. Juang, R.-S., C. Huang, and C.-L. Hsieh, *Surface modification of PVDF ultrafiltration membranes by remote argon/methane gas mixture plasma for fouling reduction.* J. Taiwan Inst. Chem. Eng., 2014. **45**(5): p. 2176-2186.

21. Khulbe, K.C., C. Feng, and T. Matsuura, *The art of surface modification of synthetic polymeric membranes.* Journal of Applied Polymer Science, 2010. **115**(2): p. 855-895.

22. Nidal Hilal, M.K., Chris J.Wright, *Membrane Modification Technology and Applications*. Vol. 1. 2012, Florida, U.S: CRC Press.

23. Tompkins, B.D. and E.R. Fisher, *Evaluation of polymer hydrophobic recovery behavior following H_2O plasma processing.* Journal of Applied Polymer Science, 2015. **132**(20).

24. Mariana, G., et al., *Surface cross linking and functionalization of poly(ethylene terephthalate) in a helium discharge.* Plasma Sources Sci. Technol., 1997. **6**(1): p. 8.

25. Kim, E.-S. and B. Deng, *Effect of NH_3 plasma on thin film composite membrane: relationship of membrane and plasma properties.* Membrane Water Treatment, 2013. **4**(2): p. 109-126.

26. Kim, E.-S., Q. Yu, and B. Deng, *Plasma Surface Modification of Nanofiltration (NF) Thin-Film Composite (TFC) Membranes to Improve Anti Organic Fouling.* Appl. Surf. Sci., 2011. **257**(23): p. 9863-9871.

27. Reis, R., et al., *Amine enrichment of thin film composite membranes via low pressure plasma polymerization for antimicrobial adhesion.* ACS Appl Mater Interfaces, 2015. **7**(27): p. 14644-53.

28. Saxena, N., et al., *Flux enhancement by argon–oxygen plasma treatment of polyethersulfone membranes.* Separation and Purification Technology, 2009. **70**(2): p. 160-165.

29. Arefi-Khonsari, F. and M. Tatoulian, *Plasma Processing of Polymers by a Low-Frequency Discharge with Asymmetrical Configuration of Electrodes*, in *Advanced Plasma Technology*. 2008, Wiley-VCH Verlag GmbH & Co. KGaA. p. 137-174.

30. Tompkins, B.D., J.M. Dennison, and E.R. Fisher, *H2O plasma modification of track-etched polymer membranes for increased wettability and improved performance.* Journal of Membrane Science, 2013. **428**: p. 576-588.

31. u, L., et al., *Surface hydrophilic modification of RO membranes by plasma polymerization for low organic fouling.* Journal of Membrane Science, 2011. **369**(1–2): p. 420-428.

32. Švorčík, V., et al., *Modification of surface properties of high and low density polyethylene by Ar plasma discharge.* Polymer Degradation Stability, 2006. **91**(6): p. 1219-1225.

33. Barton, D., et al., *An In Situ Comparison between VUV photon and ion energy fluxes to polymer surfaces immersed in an rf plasma.* The Journal of Physical Chemistry B, 2000. **104**(30): p. 7150-7153.

34. Friedrich, J., *Interaction between Plasma and Polymers*, in *The Plasma Chemistry of Polymer Surfaces*. 2012, Wiley-VCH Verlag GmbH & Co. KGaA. p. 11-33.

35. Chan, C.M., T.M. Ko, and H. Hiraoka, *Polymer surface modification by plasmas and photons.* Surface Science Reports, 1996. **24**(1–2): p. 1-54.

36. Liquori, A.M., A. Mele, and V. Carelli, *Ultraviolet absorption spectra of polyamides.* J. Polym. Sci., 1953. **10**(5): p. 510-512.

37. Švorčík, V., et al., *Ablation and water etching of poly(ethylene) modified by argon plasma.* Polym. Degrad. Stab., 2007. **92**(9): p. 1645-1649.

38. Louie, J.S., et al., *Effects of polyether–polyamide block copolymer coating on performance and fouling of reverse osmosis membranes.* J. Membr. Sci., 2006. **280**(1–2): p. 762-770.

39. Gancarz, I., G. Poźniak, and M. Bryjak, *Modification of polysulfone membranes 1. CO2 plasma treatment.* Eur. Polym. J., 1999. **35**(8): p. 1419-1428.

40. Filmtec, D. *Reverse osmosis membranes, technical manual: http://msdssearch.dow.com/PublishedLiteratureDOWCOM/dh_0042/0901b80380042dd2.pdf?filepath=liquidseps/pdfs/noreg/609-02002.pdf (accessed in July 2015).*

41. Friedrich, J., *The plasma chemistry of polymer surfaces advanced techniques for surface design*. 2012: Weinheim : Wiley-VCH.

42. Blais, P., D.J. Carlsson, and D.M. Wiles, *Surface changes during polypropylene photo-oxidation: A study by infrared spectroscopy and electron microscopy.* Journal of Polymer Science Part A-1: Polymer Chemistry, 1972. **10**(4): p. 1077-1092.

43. Prohaska, G.W., E.D. Johnson, and J.F. Evans, *Preparation and characterization of plasma-polymerized styrene thin films.* Journal of Polymer Science: Polymer Chemistry Edition, 1984. **22**(11): p. 2953-2972.

44. Friedrich, J., *Bulk, Ablative, and Side Reactions*, in *The Plasma Chemistry of Polymer Surfaces*. 2012, Wiley-VCH Verlag GmbH & Co. KGaA. p. 145-195.

45. Pawde, S.M. and K. Deshmukh, *Surface characterization of air plasma treated poly vinylidene fluoride and poly methyl methacrylate films.* Polym. Eng. Sci., 2009. **49**(4): p. 808-818.

46. Tang, C.Y., Y.-N. Kwon, and J.O. Leckie, *Effect of membranes chemistry and coating layer on physiochemical properties of thin film composite polyamide ro and nf membranes: II membrane physiochemical properties and their dependence on polyamide and coating layers.* Desalination, 2009. **242**(1–3): p. 168-182.

47. Wavhal, D.S. and E.R. Fisher, *Modification of porous poly(ether sulfone) membranes by low-temperature CO2-plasma treatment.* Journal of Polymer Science Part B: Polymer Physics, 2002. **40**(21): p. 2473-2488.

48. Chen, H. and G. Belfort, *Surface modification of poly(ether sulfone) ultrafiltration membranes by low-temperature plasma-induced graft polymerization.* Journal of Applied Polymer Science, 1999. **72**(13): p. 1699-1711.

49. Fujioka, T., et al., *Rejection of small and uncharged chemicals of emerging concern by reverse osmosis membranes: The role of free volume space within the active skin layer.* Separation and Purification Technology, 2013. **116**: p. 426-432.

50. Kim, S.H., S.-Y. Kwak, and T. Suzuki, *Positron Annihilation Spectroscopic Evidence to Demonstrate the Flux-Enhancement Mechanism in Morphology-Controlled Thin-Film-Composite (TFC) Membrane.* Environmental Science & Technology, 2005. **39**(6): p. 1764-1770.

51. Al-Jeshi, S. and A. Neville, *An investigation into the relationship between flux and roughness on RO membranes using scanning probe microscopy.* Desalination, 2006. **189**(1–3): p. 221-228.

52. Hirose, M., H. Ito, and Y. Kamiyama, *Effect of skin layer surface structures on the flux behaviour of RO membranes.* J. Membr. Sci. , 1996. **121**(2): p. 209-215.

53. Coates, J., *Interpretation of Infrared Spectra, A Practical Approach*, in *Encyclopedia of Analytical Chemistry*. 2006, John Wiley & Sons, Ltd.

54. Tse, K.C.C., F.M.F. Ng, and K.N. Yu, *Photo-degradation of PADC by UV radiation at various wavelengths.* Polymer Degradation and Stability, 2006. **91**(10): p. 2380-2388.

55. Yasuda, H., et al., *ESCA study of polymer surfaces treated by plasma.* J. Polym. Sci., Part A: Polym. Chem., 1977. **15**(4): p. 991-1019.

56. Tang, C.Y., Y.-N. Kwon, and J.O. Leckie, *Effect of membrane chemistry and coating layer on physiochemical properties of thin-film composite polyamide RO and NF membranes: I. FTIR and XPS characterization of polyamide and coating layer chemistry.* Desalination, 2009. **242**(1–3): p. 149-167.

57. Dufour, T., et al., *Chemical mechanisms inducing a dc current measured in the flowing post-discharge of an RF He-O 2 plasma torch.* Plasma Sources Sci. Technol., 2012. **21**(4).

58. Kubiak, K., et al., *Wettability Versus Roughness of Engineering Surfaces.* Wear, 2011. **271**(3): p. 523-528.

59. Holmes-Farley, S.R., C.D. Bain, and G.M. Whitesides, *Wetting of functionalized polyethylene film having ionizable organic acids and bases at the polymer-water interface: relations between functional group polarity, extent of ionization, and contact angle with water.* Langmuir, 1988. **4**(4): p. 921-937.

60. Kull, K.R., M.L. Steen, and E.R. Fisher, *Surface modification with nitrogen-containing plasmas to produce hydrophilic, low-fouling membranes.* Journal of Membrane Science, 2005. **246**(2): p. 203-215.

61. Wavhal, D.S. and E.R. Fisher, *Hydrophilic modification of polyethersulfone membranes by low temperature plasma-induced graft polymerization.* Journal of Membrane Science, 2002. **209**(1): p. 255-269.

62. Kang, G., et al., *Surface Modification of a Commercial Thin Film Composite Polyamide Reverse Osmosis Membrane by Carbodiimide-Induced Grafting with Poly(ethylene glycol) Derivatives.* Desalination, 2011. **275**(1–3): p. 252-259.

63. Van Wagner, E.M., et al., *Surface Modification of Commercial Polyamide Desalination Membranes Using Poly(ethylene glycol) Diglycidyl Ether to Enhance Membrane Fouling Resistance.* Journal of Membrane Science, 2011. **367**(1–2): p. 273-287.